Available online at www.sciencedirect.com
SCIENCE DIRECT®
C. R. Physique 6 (2005) 415–429
COMPTES RENDUS PHYSIQUE
http://france.elsevier.com/direct/COMREN/

Aircraft trailing vortices/Tourbillons de sillages d'avions

Experimental investigations on wake vortices and their alleviation

Ömer Savaş

Department of Mechanical Engineering, University of California at Berkeley, Berkeley, CA 94720-1740, USA

Available online 5 July 2005

Abstract

Recent wake vortex research in the laboratory has benefited considerably from concurrent analytical and numerical research on the instability of vortex systems. Tow tank, with dye flow visualization and particle image velocimetry is the most effective combination for laboratory research. Passive and active wake alleviation schemes have been successfully demonstrated in the laboratory. The passive alleviation systems exploit the natural evolution of vortex instabilities while the active systems rely on hastening selected instabilities by forcing the vortices individually or as a system. Their practical applicability, however, will have to meet further criteria beyond those dictated by fluid dynamics. ***To cite this article: Ö. Savaş, C. R. Physique 6 (2005).***

Résumé

Recherches sur les tourbillons de sillage et leur contrôle. Les recherches actuelles en laboratoire sur les tourbillons de sillage s'appuient largement sur les avancées récentes dans le domaine de l'analyse théorique des écoulements tourbillonnaires (stabilité) et sur les progrès réalisés dans le domaine de la simulation numérique. La traction de maquettes dans un bassin hydrodynamique, associée à des mesures PIV (Particle Image Velocimetry), constitue probablement la méthode expérimentale la plus efficace pour ce type d'études. Des méthodes de contrôle passif et actif visant à réduire l'intensité des tourbillons ont été testées avec succès dans ce type d'installation. Le contrôle passif exploite le caractère intrinsèquement instable de configurations de tourbillons engendrées par des plans de voilure particuliers. Le contrôle actif consiste à forcer les modes d'instabilités dominants. Ces méthodes sont efficaces, mais leur mise en pratique soulève un certain nombre de problèmes qui sont discutés ici et qui ne relèvent pas que de la mécanique des fluides. ***Pour citer cet article : Ö. Savaş, C. R. Physique 6 (2005).***

Keywords: Wake vortex; Alleviation; Passive alleviation; Active alleviation; Vortex experiments

Mots-clés : Tourbillon de sillage ; Contrôle ; Contrôle passif ; Contrôle actif ; Recherches sur les tourbillons de sillage

1. Introduction

Experimental investigations [1–3] into wakes of lifting airfoils began as scientific curiosities to confirm Lanchester's ideas (§126, 127 of [4]) that after *"the aerofoil has passed there exists a Helmholtz surface of gyration"*, that *"this surface of gyration will, owing to viscosity, break up into a number of vortex filaments or vortices"*, and that these *"vortex filaments will evidently wind around one another"* forming *"two vortex trunks"* with opposite rotations. Now, however, it has become a question of safety and safe economics. Soon after the introduction of the large aircraft (B-747) into service, there was a period of intense

E-mail address: savas@me.berkeley.edu (Ö. Savaş).

1631-0705/$ – see front matter
doi:10.1016/j.crhy.2005.05.004

Nomenclature

Symbol	*Description*
b	wing span
b_f	wing span of a following aircraft
c	chord
d	vortex separation
f	frequency
$\dot{m}$	mass flow rate
r	radial coordinate
r_{EN}	enstrophy dispersion radius, $[\int r^2\omega^2\,\mathrm{d}A/\int \omega^2\,\mathrm{d}A]^{1/2}$
x, y, z	coordinate axes, defined in Fig. 1(e)
w	velocity component in z direction in the vortex wake
$\mathcal{D}$	binary molecular diffusion coefficient
D	$\int_b w(y')\,\mathrm{d}y'/b$, surrogate for downwash on an aircraft in wake
R	$\int_b y'w(y')\,\mathrm{d}y'/b$, surrogate for rolling moment on an aircraft in wake
M	rolling moment on following aircraft
S	wing area
U	free stream velocity, towing velocity
U_j	jet velocity
α	angle of attack
$\alpha_{\max}$	dimensionless maximum growth rate
γ	circulation strength ratio of a vortex pair, $[-1, 1]$
γ_t	circulation strength ratio of tail vortex versus wing tip vortex
λ	wave length
ρ	density
ν	kinematic viscosity
σ	vortex core radius
τ	dimensionless wake descent time
τ_p	dimensionless vortex pinching time
ω	axial vorticity
Γ	circulation, vortex strength
Γ_h	strength of reference horseshoe vortex system for following aircraft
Ω	average angular velocity
C_L	lift coefficient of generating (leading) aircraft
$C_{\dot{m}}$	mass flow rate coefficient, $\dot{m}/\rho SU$
C_μ	momentum flow rate coefficient, $2\dot{m}U_j/\rho SU^2$
C_M	rolling moment coefficient on following aircraft, $2M/\rho bSU^2$
Re_c	chord based Reynolds number, Uc/ν
Re_Γ	circulation based Reynolds number, $\Gamma/\nu \approx C_L US/2\nu b$
Sc	Schmidt number, $\nu/\mathcal{D}$

research activity on the nature of the vortex wake of those aircraft as evidenced by the flurry of papers and notable symposia three decades ago [5–7]. Continually increasing air traffic and the introduction of an even larger aircraft (A-380, maiden flight on 27 April, 2005) have now reignited the wake vortex capacity and safety issues, specialty conferences and review articles have now come the fore [8–13] as well as an up-to-date online bibliography [14].

Fig. 1 is a pictorial synopsis of the wake vortex issue. The first flight of Boeing-747 in 1969 photographed in Fig. 1(a) ushered in the era of jumbos jets [15]. In the series of photographs in Fig. 1(b), water entrained in cores makes visible the vortices in the far wake of an airplane flying at cruise altitude [16]. Both short- and long-wave instabilities are evident. The vortex filaments eventually form Crow rings [17], losing their coherent filamental structure. The circulation based Reynolds number Re_Γ is $\mathcal{O}(10^7)$. A 0.01 scale model of a B-747 aircraft in take-off configuration with its landing gear down is shown in Fig. 1(c) and its near vortex wake visualized in a towing tank in Fig. 1(d) [18]. The dye patches in the Treftz plane mark the co-rotating vortices formed off the wing and flap tips whose interaction and eventual mergers to a single pair of counter-rotating vortices depend strongly on the wake of the landing gear. Re_Γ based on the estimated root circulation of the model is $\mathcal{O}(10^5)$. Fig. 1(e) is a generic airplane configuration where two rectangular planform cambered wings are used to model the wing-tail combination of an airplane [19]. A sample dye visualization picture of the interaction of the counter-rotating vortex pair on one side of its vortex wake is shown in Fig. 1(f). The respective lift forces on the wing and tail components are such that the resulting circulation ratio results in a vigorous instability mode as evidenced by the wrapping of the weaker tail tip vortex around the wing tip vortex. Re_Γ is $\mathcal{O}(10^5)$. Fig. 1(g) shows the three wing models (rectangular planform, central flapped, and outboard flapped) used in the tow tank experiments by [16,20–22]. A snapshot of the complete wake off the outboard flapped wing is shown in Fig. 1(h). Dye traces indicate a vigorous instability in the wake. Re_Γ is $\mathcal{O}(10^5)$.

The decreasing degree of complexity in the vortex wakes generated behind the flow models in Figs. 1(a), (c), (e), (g) respectively generate increasingly tractable flow fields. The ultimate goal still remains to engineer the wake of the class of aircraft in Fig. 1(a), for the purposes of both airport capacity and air travel safety. The experiments conducted using model test have been at Reynolds numbers more than two orders of magnitude lower than the real one. Hence, there is an issue of incomplete similarity: how does one extend the instability behavior observed at lower Reynolds numbers to full scale conditions? Even more basic, are these modes of instability still the optimum modes at full Reynolds numbers?

Left alone, the vortex wake off a singly-connected wing-like lifting body will end up as a pair of equi-strength counter-rotating vortices whose eventual demise comes through development of instabilities if the Re_Γ is sufficiently high. The nature

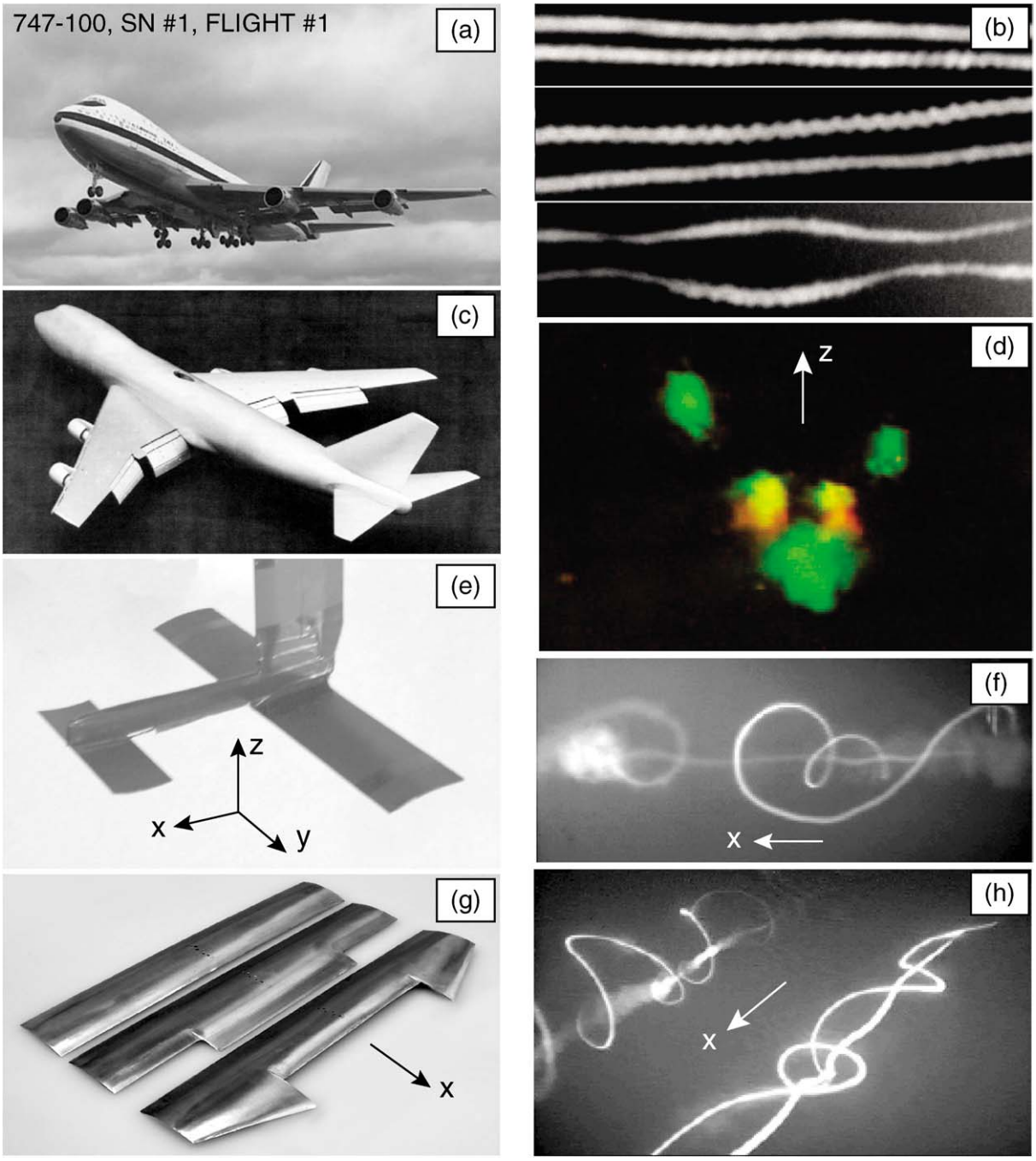

Fig. 1. (a) A large airplane [15], (c) its 1:100 scale model [18], (e) a wing-and-tail generic airplane model [19], (g) three sheet metal wing models: rectangular planform, with a contiguous inboard flap, and with outboard triangular flaps (TF) [16,21] (left column, top to bottom) and their respective vortex wake images (right column): a pictorial illustration of the simplification needed for laboratory experiments for mechanical manageability and analytical tractability. Re_Γ is $\mathcal{O}(10^8)$ for the large airplane in (b) and $\mathcal{O}(10^5)$ for the laboratory model flows in (d), (f), (h) (see Tables 1 and 2).

of the instabilities depends, primarily, on the vortex separation, and, secondarily, on vortex structure, including vorticity distribution and axial flow when in homogeneous quiescent medium. A typical vortex separation for commercial air transport is $b/\sigma \sim 10$ [68,70], for which the Crow instability is the mechanism that alters the wake from filamental structure to ring

structure. This mode takes rather long times to mature. If one desires to render the wake benign quicker, either by accelerating its natural demise or by destroying its internal structure such that its undesirable effects are mitigated, one may accelerate the evolution of the Crow instabilities by forcing, force changes in the vortex structure to alter its nature all together, or redesign the vortex wake from the beginning. Crow himself proposed a forcing scheme using the control surfaces of a wing to hasten the development of cooperative instabilities of the counter-rotating vortex pair in its wake [23]. Bilanin and Widnall explored this concept in their tow tank experiments [24]. These experiments, however, were not carried out far enough in the wake to observe the implications for eventual ring formation. To achieve this stated goal, one should revisit the older ideas under the light recent of theoretical developments and at the same time explore unusual, even radical avenues. For example, insisting on a long list of things that one must strive to intensify, e.g., the turbulence near the core, the helical instabilities at the edge of the vortex, the axial velocity, may not be an optimum approach. Dunham [25] describes a list of initially tested concepts, including mass injection, oscillating devices, wing tip modifications, vortex interactions, and end plates. None of these however resulted in a practical solution on the affect of the wake on a following aircraft. For example, Corsiglia et al. [26] describe a set of experiments followed by flight tests where a vortex dissipater mounted near the wing tip of a leading aircraft resulted in a somewhat tamer vortex, even though its useful effects on a following aircraft remained elusive. Despite a lack of success, one must not rush to ignore these ideas, for it is quite possible that explored parameter spaces may have been just too small to reach any meaningful conclusions. The researchers then did not have access to theoretical and experimental tools that are available now for exploring the parameter spaces.

Experiments are made under carefully controlled environments, mostly quiescent and unstratified conditions, whereas tests are done almost never at these conditions. It is well known that turbulence, stratification, and wind shear have profound effects on the behavior of vortex filaments, both individually and in groups. Further, the laboratory experiments are conducted at Reynolds numbers at least two orders of magnitude lower than tests. Hence, there is the issue of extending lower Re_Γ laboratory results to test conditions.

Experiments and test are exact realizations at their respective conditions; any uncertainty is either a reflection of interpretation of results or inadequacy of instrumentation. Comparison of experiment and test with numerical calculations are inevitable. On one hand, the Reynolds number for exact calculations are too low to be useful. The modeling used to simulate high Reynolds numbers, on the other hand, is still evolving. We must therefore, be judicious on interpollination of ideas among experiments, test, and computations. Advances in LES computations of vortex interactions have been extremely promising [13].

The purpose of this paper is to review laboratory experiments on wake vortex, with the emphasis being on alleviation. Some of the notable experiments are tabulated in Tables 1 and 2 to provide a quick guide. Flow generation techniques, instrumentation and data analysis are discussed. Passive and active wake alleviation schemes are taken up and a critique is provided. The paper concludes with some parting thoughts.

2. Experimental vortex wake

2.1. Flow generation

Tables 1 and 2 list some experiments on wake vortex structure, interaction, and alleviation. They are not exhaustive, yet representative of the work done currently, as well as four decades ago. They list in the alphabetic order of investigator(s), flow facility, instrumentation, and flow generators used in the experiments. The numerical entries in Table 2 are the maxima noted in or estimated from the reference. The short remark in the last column of Table 2 indicates the most relevant aspect of the work for the purpose of this review paper. No experiments in stratified media are listed.

Experiments have employed models ranging from high-fidelity models of large aircraft to simple sheet metal wings (Fig. 1). Particular choices are dictated by any, or combinations of reasons, such as cost, Reynolds number, geometrical similarity, scientific tractability, isolation of specific aspects. At low Reynolds numbers, especially below $\mathcal{O}(10^5)$, cambered sheet metal airfoils are most effective, primarily due to prevention of laminar boundary layer separation at high angles of attack [74]. The use of the popular NACA-0012 or thicker profiles requires boundary layer tripping if high angles of attacks are used. The same is also true for aircraft replicas.

When the goal is the interaction of vortices alone, whether they are generated off a single wing (with or without flaps) or half wings arranged as multiple vortex generators, is of secondary concern. If the goal is the dynamics of the vortex wake of a lifting body, then the relevance of a vortex system generated off multiple independent vortex generators to that in the wake of a single body must be examined closely. The particulars of the wrapup of the vortex sheet into filaments depend on the flow over the generators. Thus, the embedded disturbances in the wakes of single lifting bodies are bound to be different than those of multiple generators. Such disturbances will have different effects of the development of instabilities in the system. For example, the intervening fluid between two counter rotating vortices generated off two half wings is initially free of disturbances except

the induced motion whereas that between those generated off a single wing contains perturbations off the upper and lower surface boundary layers of the wing.

Simulation of a full wake with the wake of a half-body has to be viewed critically also. For short downstream distances and thin vortices ($\sigma/b \ll 1$), simulation is acceptable. For example, the initial phases of Crow instability of a counter rotating vortex pair may be described adequately by the behavior of a single vortex over a plane. As the instability evolves, and the ring formation process becomes imminent, the secondary vorticity generated at the plane of symmetry renders the simulation irrelevant. An even more forceful demonstration is given by the flow described in Ortega et al. where vortex filaments cross the plane of symmetry [21], which would not have been possible had there been a *plane* of symmetry.

2.2. Flow facility

Wind tunnels and tow tanks are used with nearly equal frequency in vortex wake research. Both have unique strengths and shortcomings. ONERA's catapult is a remarkable exception [36]. Another exception is what we will name a *time tank*, where vortices are generated along the length of the tank in a 2D manner and are allowed to evolve in time [31,32,54,55,58,59]. In assessing the respective utility of each facility, its relative dimensions, flow characteristics, flow Reynolds numbers, and instrumentation must be considered. The essential requirement is that apparatus must allow for observation of the far field behavior of the vortex wake, i.e., $x/b \sim \mathcal{O}(10^2)$.

Wind tunnels are the easiest to operate and the most suitable for near field surveys. The instrument of choice used to be the hot wire anemometer, but this is being replaced by particle image velocimetry (PIV). Five/seven-hole probes are also robust alternatives. Visualization is done most effectively via smoke and sometimes steam injection. Tufts are used occasionally. Wind tunnel experiments are most suitable for force and moment measurements. Measurements with fixed probes are plagued by vortex meandering for which rather elaborate techniques have been devised. However, it is the instantaneous behavior of the wake that is important for the purpose of vortex alleviation. One must follow the evolution of vortex systems in real time to extract analytical information. Averaging clouds even obscures the stability behavior of the vortex system in a wake.

Flow visualization in wind tunnels using smoke is rather instructive. Since the Schmidt number is of order unity, diffusion of vorticity and smoke are nearly the same, hence diffusion of smoke closely marks the diffusion of vorticity. Therefore, smoke pictures taken in air are closer to the vorticity distribution than dye pictures taken in water, especially in the far field. We must note here that the first vortex wake visualization experiments are made in a wind tunnel by Caldwell and Fales [1]. In this ingenious approach, the wind tunnel is turned into a *fog tunnel*, and the water cloud is used as the flow visualization agent. The resulting photographs exquisitely show the vortex formation (e.g., cover page and Fig. $18\frac{1}{2}$ of [1]). Unfortunately, without the proper understanding of the flow visualization tool, the authors inadvertently reached untenable conclusions (Figs. 34a,b of [1]).

In order to reach large x/b values requisite for far wake studies, either the tunnels have to be long, or models small. If one also desires sufficiently large Reynolds numbers, then most wind tunnels fall inadequate. Therefore, useful wind tunnels experiments have been at large wind tunnels using relatively small models to achieve both moderate x/b and Re_Γ values.

Tow tanks, standard equipment for marine applications, have proven to be perhaps the most useful apparatus for vortex wake experiments ([16,18,20–22,38] and so on). Their primary advantage is the possibility of large x/b values at relatively high Reynolds numbers. PIV is the instrument of choice. Dye flow visualization has proven to be rather remarkable. However, there is a stark contrast between dye flow visualization in a water towing tank and smoke flow visualization in a wind tunnel. Due to the rather large Schmidt number of the binary diffusion of species in liquids, diffusion of dye lags that of vorticity. Hence, all dye marks vorticity, whereas not all vorticity is marked by dye. Therefore, one must exercise due caution when comparing and interpreting smoke and dye flow visualizations.

One word of caution, when the towed model is stopped, a soliton propagates back in vortex cores. One must be careful not to contaminate observations. This is especially a point of concern in short tow tanks where elapsed time t is taken as a surrogate for downstream distance x. One should either continue towing until observations are finished or terminate observations when the soliton arrives at observation site. Either approach may require some trial and error, and is recognized by many researchers.

2.3. Instrumentation

Flow visualization is the most effective tool and must be employed first whenever feasible. Dye marks vorticity, but not all vorticity is marked by dye. Since the Schmidt number Sc is $\mathcal{O}(10^2)$ for a typical dye–water combination, the dye remains intact, oblivious to the viscous diffusion. Smoke visualization in air is a better indicator of vorticity diffusion since Sc is of order unity.

Tracers can be misleading: all one has to do is to take a look at plates 16 (Figs. 39, 40) and 24 (Figs. 59, 60) of Prandtl and Teitjens [75]. Identification of a vortex, especially its apparent core from streaklines depends on whether the vortices are moving

Table 1
Summary of experiments, continues to the right into Table 2

Investigators	[Ref. #]	Flow facility	Instrumentation	Model(s)
Baker et al.	[27]	open water tunnel	LDV	circular arc lens hydrofoils
Bandyopadhyay et al.	[28]	wind tunnel	7HP, sFV, HW	half-wings, NACA-0012
Bilanin, Widnall	[24]	tow tank	dFV	wing, 0.1 thickness ratio
Bilanin et al.	[29]	wind tunnel (V-STOL)	sFV, HW	model, NACA-0018
Brant, Iversen	[30]	wind tunnel	sFV, HW, SG	half-wings, NACA-0012
Bristol et al.	[16,22]	tow tank	dFV, PIV	cambered thin wings
Caldwell, Fales	[1]	wind tunnel	fFV, Toledo scales	flat-bottom propeller sections
Cerretelli, Williamson	[31,32]	tow tank	PIV	two thin half-wings
Chen et al.	[33]	tow tank	PIV	cambered thin wing
Ciffone, Lonzo	[18]	tow tank	dFV	B747 model (0.01)
Ciffone, Orloff	[34]	tow tank	scanning LDV	wing, NACA-0015
Corsiglia et al.	[35]	wind tunnel	sFV, rotating HW	wings, NACA-0015
Coton	[36]	catapult	DGV, sFV, HeBB	A300B2 model (1/22)
Croom	[37]	wind tunnel (V-STOL)	balance	B747 model (0.03)
Crouch et al.	[38]	tow tank	dFV, balance	generic airplane model
Czech et al.	[39]	wind tunnel	5HP, dFV	generic airplane model
de Bruin et al.	[40]	wind tunnel	5HP, sFV	generic model
Devenport et al.	[41–43]	wind tunnel	HW	half-wing(s) NACA-0012
Durston et al.	[19]	tow tank	dFV, PIV	generic airplane model
Fage, Simmons	[3]	wind tunnel	HW, PT	wing, R.A.F.6a
Graham	[44–46]	tow tank	FV, PIV	thin half-wing, notched wing
Haverkamp et al.	[47]	tow tank	PIV	wing, NACA-0012
Heyes, Smith	[48]	wind tunnel	HW, PIV	half-wing, NACA-0012
Jacob et al.	[49–51]	tow tank	dFV, PIV	wing, NACA-0012
Jacquin et al.	[52,53]	wind tunnel	sFV, HW, LDV	A300 model (1:100)
Laporte, Leweke	[54]	time tank	dFV, PIV	flaps
Leweke, Williamson	[55]	time tank	dFV, PIV	flaps
Lezius	[56]	tow tank	FV, HBB	wing, NACA-0015
Li, Jacob	[57]	tow tank, wind tunnel	7HP, PIV	half wings, NACA-0012
Meunier, Leweke	[58]	time tank	dFV, PIV	two flaps
Meunier, et al.	[59]	time tank	dFV, PIV	flaps
Olsen	[60]	tow tank	dFV	strut, NACA-0012
Ortega et al.	[20,21,61]	tow tank	dFV, PIV	cambered thin wings
Özger et al.	[62]	wind tunnel	sFV, HW, SG	half-wing, BAC 3-11/RES/30/21
Piercy	[2]	wind channel	PT	wing, R.A.F.19
Quackenbush et al.	[63]	water tunnel	balance	deformable half wing
Patterson et al.	[64–66]	Langley track	sFV, SG	Aircraft models (0.03, 0.07)
Rossow et al.	[67]	wind tunnel	balance	B747 model (0.03)
Sarpkaya	[68]	tow tank	dFV, PIV	wing, NACA-0012
Schell et al.	[69]	wind tunnel	HW, SG	half-wing, Eppler-1232
Spreiter, Sacks	[70]	water tank	aluminum flakes	flat plate wings
Thompson	[71]	tow tank	HBB	wings, NACA-0012, 6412
Vollmers et al.	[72,73]	tow tank	sFV, PIV	generic airplane model

5HP—five hole probe, 7HP—seven hole probe, DGV—Doppler global velocimetry, (d/f/s)FV—(dye/fog/smoke/steam) flow visualization, HBB—hydrogen bubble, HeBB—helium bubble, HW—hotwire/film anemometry, LDV—laser Doppler velocimetry, PIV—particle image velocimetry, PT—pressure tube, SG—strain gage balance, SMA—shape memory alloy, n/a—not available/applicable.

with respect to the observer. Another instructive example is discussed by Delisi and Greene on how different flow visualization techniques can lead to different conclusions [76]. The correct identification must be made as the vorticity centroid (see, for example, Fig. 4 of [33]).

The most suitable laboratory instrument for vortex research is PIV. Implementation of the basic 2D version is straightforward. Three-D implementation poses some difficulty, yet it is invaluable, since it yields axial flow information in vortex core that has strong influence on stability behavior. In addition to providing instantaneous field data, it has also removed the ambiguities associated with vortex meandering (see, for example, [27,41–43]). One point of caution is that high deformation rates of vortices poses challenges to PIV algorithms and iterative data processing may be better suited for analysis of PIV images [33,77]. Laser-Doppler velocimeter (LDV) is currently the only relatively non-intrusive, high frequency-response probe

Table 2
Summary of experiments, continued sideways from Table 1

Investigators	[Ref. #]	Re_c	Re_Γ	x/b	Remarks
Baker et al.	[27]	70,000	10,000	9.7	vortex structure
Bandyopadhyay et al.	[28]	100,000	20,000	9.2	vortex structure in turbulent stream
Bilanin, Widnall	[24]	131,000	31,000	32	differentially oscillated flaps
Bilanin et al.	[29]	440,000	220,000	7.5	model verification
Brant, Iversen	[30]	460,000	630,000	15(!)	vortex merger
Bristol et al.	[16,22]	335,000	210,000	65	merger, stability
Caldwell, Fales	[1]	340,000	160,000	$\mathcal{O}(10)$	first wake vortex visualization
Cerretelli, Williamson	[31,32]	5,700	1,665	n/a	vortex merger
Chen et al.	[33]	82,000	64,000	52	vortex merger
Ciffone, Lonzo	[18]	175,000	176,000	22	multiple vortex interactions
Ciffone, Orloff	[34]	240,000	n/a	190	axial flow in vortices
Corsiglia et al.	[35]	840,000	350,000	31	dissipator panel
Coton	[36]	360,000	290,000	93	unique experiment
Croom	[37]	n/a	n/a	45	spoilers as attenuators
Crouch et al.	[38]	600,000	500,000	80	active alleviation scheme
Czech et al.	[39]	600,000	500,000	10	active alleviation scheme
de Bruin et al.	[40]	540,000	540,000	5	near field wake survey
Devenport et al.	[41–43]	530,000	190,000	7.5	vortex structure, merger
Durston et al.	[19]	320,000	170,000	280	passive alleviation scheme
Fage, Simmons	[3]	155,000	64,000	2.2	first wake vorticity measurement
Graham	[44–46]	53,000	18,000	20	persistent vortex pair
Haverkamp et al.	[47]	50,000	37,000	60	wake alleviation
Heyes, Smith	[48]	220,000	37,000	n/a	pulsed jet
Jacob et al.	[49–51]	37,000	60,000	175	pulsed jets
Jacquin et al.	[52,53]	200,000	170,000	9	wake formation and development
Laporte, Leweke	[54]	n/a	2,800	n/a	counter-rotating pair instability
Leweke, Williamson	[55]	n/a	2,800	n/a	counter-rotating pair instability
Lezius	[56]	750,000	150,000	242	vortex decay
Li, Jacob	[57]	240,000	46,700	3.7	vortex merger
Meunier, Leweke	[58]	n/a	4,000	n/a	vortex merger
Meunier, et al.	[59]	n/a	2,300	n/a	2D merger, equistrength corotating pair
Olsen	[60]	31,000	n/a	n/a	vortex core stability, mutual instability
Ortega et al.	[20,21,61]	330,000	110,000	350	passive wake alleviation
Özger et al.	[62]	800,000	430,000	1.0	wake structure, passive alleviation
Piercy	[2]	65,000	25,000	n/a	first wake vortex structure measurement
Quackenbush et al.	[63]	1,600,000	310,000	n/a	SMA actuator demonstration
Patterson et al.	[64–66]	520,000	360,000	27	wing tip devices, thrust reverser
Rossow et al.	[67]	660,000	610,000	13.8	vertical fin on wing
Sarpkaya	[68]	n/a	90,000	n/a	vortex decay arguments
Schell et al.	[69]	300,000	320,000	1.0	wake structure, passive alleviation
Spreiter, Sacks	[70]	n/a	n/a	2	vortex sheet roll up
Thompson	[71]	68,000	20,000	18	axial flow in vortex
Vollmers et al.	[72,73]	100,000	n/a	28	Rayleigh–Fjørtoft–Ludwieg instability

Reported or estimated maximum numerical values are shown. The last column notes the most relevant aspect for the purpose of this review paper.

available. Being a point-wise technique makes it less attractive. Also, slight mismatches in fluid and seed particle density biases the velocity measurement at vortex cores due to high centrifugal accelerations. Since the vortices are extremely temperamental, measurement made with intrusive probes (hot wire, pressure probes, tracers with overly mismatched densities) do alter the very vortex structure one is trying to determine. Five and seven hole probes are robust instruments for mapping 3D mean velocity field in wind tunnel, especially suitable for mapping near vortex field. They suffer, however, from the vortex meandering problem.

The ultimate measure of wake alleviation is the downwash and rolling moment experienced by the following aircraft. The best quantification is the balance in the laboratory. Their use in wind tunnel is prolific, but difficult for tow tank implementation. An alternative is the approach Rossow has developed where the velocity field is used to estimate the downwash and the rolling

moment, which has been shown to be a reliable alternative to the balance [78]. In this approach, the integrals D and R are used as surrogates for downwash and rolling moment on a following aircraft, respectively.

3. Controlling an evolving vortex wake

A single vortex filament or collection of filaments exhibit various modes of instabilities, driven by either the internal distribution of vorticity in a filament or mutual interactions among filaments or combinations of both. A single vortex can exhibit internal modes of varying shapes, which can manifest as sinus, varicose, helical, or centrifugal instabilities [79]. Multiple vortex systems exhibit numerous instabilities; the Crow instability between equip-strength counter rotating pair [17] and its generalization to unequal strength counter rotating vortex pairs [22], multiple modes of instability in symmetric co-rotating pairs [80,81], and multiple modes of instability in symmetric counter-rotating pairs [16,82]. Any laboratory or field vortex system is likely to have embedded perturbations that may be in tune with one or many of these modes. Passive alleviation systems exploit the natural evolution of the instability modes with the highest growth rates while active systems rely on hastening selected modes of instability by forcing the vortices individually or as a system. The passive system is essentially a vortex wake design endeavor, while an active system is an actuator design project.

Dunham describes a list of exploratory concepts, active and passive, that were investigated by NASA in 1970s [25]. Although there were some successes, no practical solution emerged based on those investigations, which seem to have been based largely on educated guesses, therefore limited in their respective parameter spaces. Developments in analytical, computational and experimental tools during the intervening years have now made it possible to propose concepts based on fundamentals of vortex dynamics that are viable. Not only are we able to better explain observations, but also we are now able to design practical systems. There are now available laboratory demonstrated schemes of alleviating the wake vortex, passive and active, and both based on firm fundamental vortex dynamics.

4. Passive schemes

4.1. Cooperative instability

Fig. 2 shows the highlights of the passive wake vortex alleviation scheme demonstrated at Berkeley, which exploits the explosive growth rate of the cooperative instabilities between unequal strength counter rotating vortices [20,21,61]. This growth rate for the most unstable perturbation amplitudes is shown in Fig. 2(a) for the weaker vortex of a pair as a function of the vortex strength ratio γ and vortex separation σ/d [16]. The instability behavior of a counter rotating pair in a symmetric four-vortex system remains nearly the same if the separation distance between the pairs is sufficiently larger than that between the vortices of a pair. Laboratory experiments showed that a four-vortex system comprising of two symmetric vortex pairs of circulation strength ratio of $\gamma \sim -0.4$ generates the most desirable flow for wake vortex alleviation. The particular implementation at the UC California, Berkeley tow tank at Richmond Field Station is done by using a wing with outboard triangular flaps (Fig. 1(d)), adding extra lift outboard to generate the desired counter rotating vortex pairs. A snapshot of the ensuing vortex interaction, as visualized by fluorescent dye is shown in Fig. 1(h) [21]. The resulting nonlinear interactions between the vortices result in a wake that is highly three-dimensional and incoherent. The frame is populated with characteristics Ω-loops. Fig. 2(b) shows the evolution of the enstrophy dispersion radius during the evolution of the instabilities. Vorticity is suddenly redistributed to almost all across the wing span soon after the onset of the instabilities at about $x/b \sim 40$. In contrast, the vorticity in the wake of a rectangular wing remains intact for hundreds of spans behind the wing. The wake alleviation properties of these flows are quantified using data from particle image velocimetry and are shown in 2(c), (d). The ensuing redistributed vorticity field results in substantial decreases in both the rolling moment and downwash on a simulated following wing. The resulting distributions of rolling moment and downwash are shown to be highly diffuse when compared to those in the wake of the rectangular wing. Furthermore, both the maximum rolling moment and downwash are approximately one-half the average value for the rectangular wing by 75 spans. This behavior is seen to exist for all of the experimental runs over which the counter rotating flap vortices have strengths ranging from -0.4 to -0.7, most profound results being for $\gamma = -0.4$.

Figs. 1(e), (f) and 2(e), (f), reproduced from Durston et al. [19], show the implementation of the cooperative instability mechanism using a more traditional wing-tail combination modeling an aircraft. In this implementation, the counter-rotating vortex needed to incite the instability in cooperation with a tip vortex is generated by the down lift of the tail airfoil. The resulting rolling moment estimates in Fig. 2(e) are similar to those from a single wing with outboard flaps shown in Fig. 2(c). Figure 2(f) shows the time to halve the rolling moment in these experiments, which corroborates the results of Ortega et al. [20] that at $\gamma \sim -0.4$ the drop in rolling moment is the fastest.

Jacob et al.'s experiments with vertical fins on a wing and triangular flaps attached to a wing are independent confirmations of the prowess of cooperative instabilities within counter-rotation vortex pairs in altering the characteristic of vortex wakes

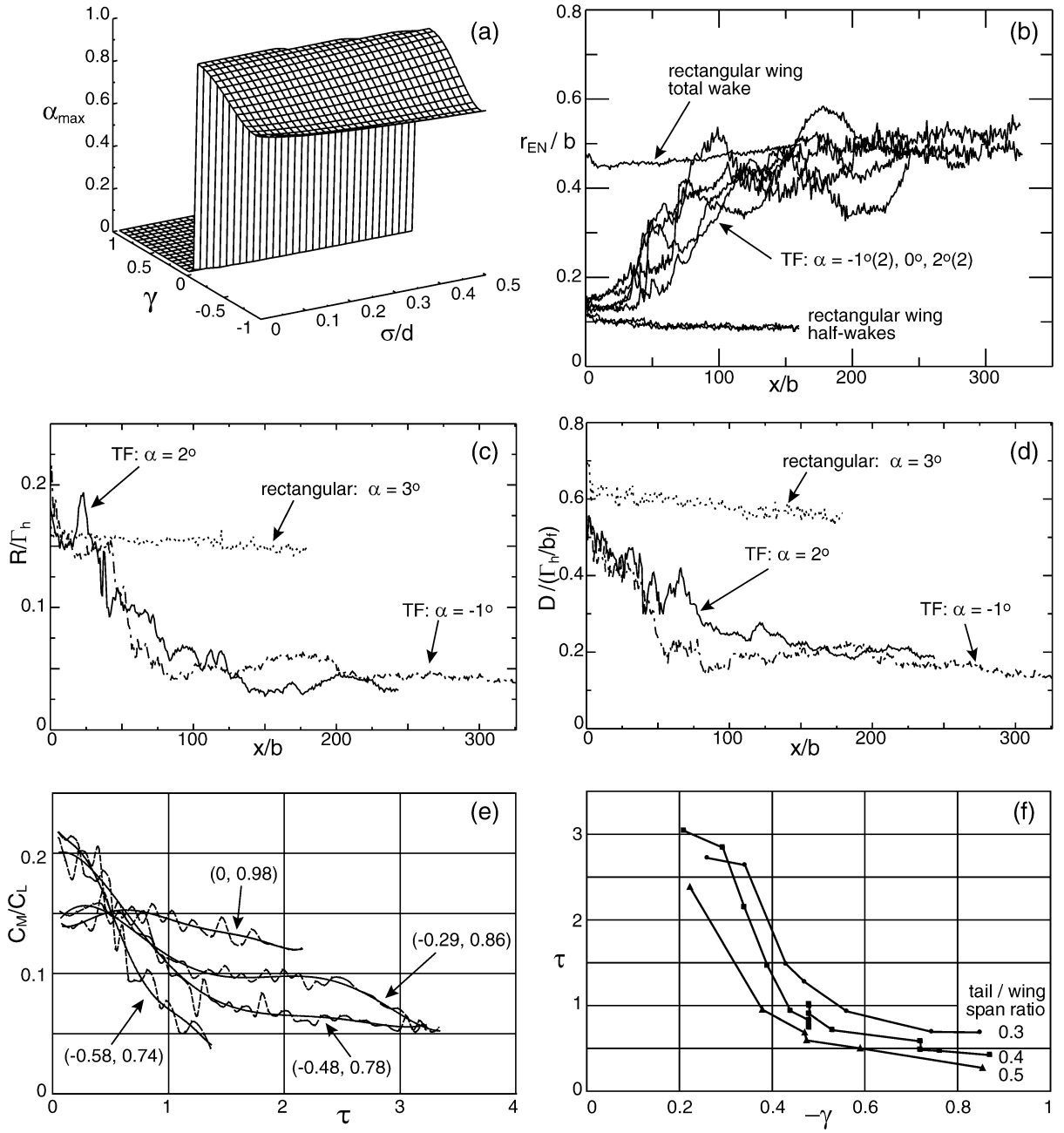

Fig. 2. Passive wake alleviation based on cooperative instabilities between counter-rotating vortex pairs. (a) the maximum growth rate of perturbation amplitudes of the weaker vortex within pair of γ [16], (b) vorticity re-distribution in the wakes of two of the models in Fig. 1(g) [21]; (c), (d) maximum rolling moment and maximum downwash on a simulated following airplane in the wakes of the rectangular and TF wings in Fig. 1(g) [20]; (e), (f) maximum rolling moment and time to halve rolling moment on a simulated following airplane in the wake of the generic airplane model in Fig. 1(e) [19]. Curves in frame (e) are labeled with their respective values of (γ, C_L).

[47,62]. In the wind tunnel experiments of Özger et al. the control vortex off a vertical fin generated sufficient interaction with the tip vortex to significantly reduce the rolling moments in the vortex wake [62]. The tow tank experiments of Haverkamp et al. [47] are essentially a corroboration of the conclusions reached by Ortega et al. [20] on the influence of outboard triangular flaps on the wake of a rectangular wing.

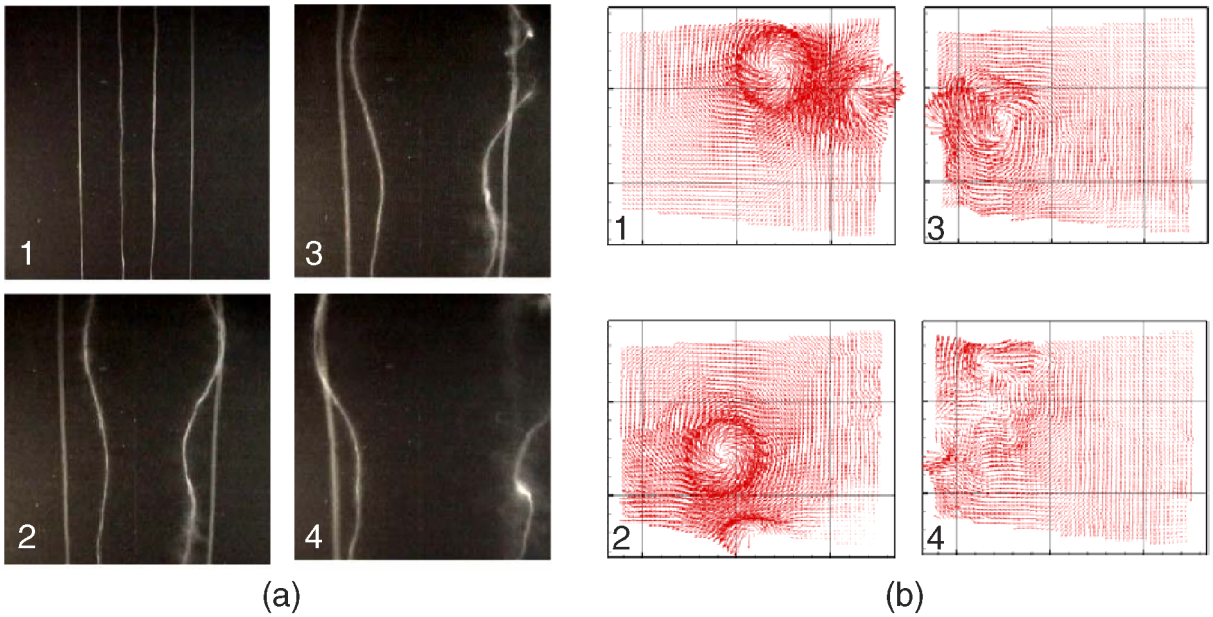

Fig. 3. Wake alleviation based on centrifugal instability of a vortex with radially alternating signs of vorticity [73] (reproduced with permission). The flow is generated by towing a generic airplane model comprising of a lifting wing a pushing trailing tail, hence a vortex wake of two symmetric counter-rotating vortex pairs of $\gamma \approx -0.5$. The numeric labels order the frames in time. (a) Dye visualization of the wake. The weaker tail vortices are wrapped around the wing vortices, non-uniformly, however. Note that the dye topology in the upper right corner of frame 3 is reminiscent of the 'feet' of the $'\Omega'$ structures in Fig. 1(h). (b) PIV measurements of half wake. At the plane of measurement, the weaker vortex orbits around the wing vortex and rapidly looses its coherence.

4.2. Centrifugal instability

An individual vortex in a wake may be induced to undergo sudden enlargement, so that its vorticity is spread over a larger area, and that area may even get so large that it starts interacting with its counter part from the other side of the wake to bring about mutual destruction. Such sudden enlargements over the entire length of vortices have not been observed in free vortices with single sign of vorticity. However, it is possible to incite this behavior if one can design a vortex by depositing at its perimeter a sufficient amount of vorticity of the opposite sign. Fjørtoft describes the instability of a vortex with decreasing as well as increasing vorticity distribution [83], and puts more a stringent requirement on its instability than that of Rayleigh. *"If all values of* (*average*) Ω *in the region with negative* $(\mathrm{d}\omega/\mathrm{d}r)$ *are greater than all values in the region with positive* $(\mathrm{d}\omega/\mathrm{d}r)$*, then as a results of the transport of the vortices of the initial mean flow, kinetic energy of the mean flow is transformed to kinetic energy of the irregular flow"* (§20 of [83]). Thus, the presence of opposite signed vorticity within a vortex offers possibility of destabilization which is further extended by Ludwieg [84]. The passive wake vortex alleviation mechanism discussed by Stuff et al. exploits this instability mechanism by wrapping oppositely signed vorticity from a tail tip around a wing tip vortex [85,86].

Fig. 3 shows results from recent experiments exploiting Rayleigh–Fjørtoft–Ludwieg radial instability [73]. The sequence of photographs show the evolution of a four-vortex system generated off a generic airplane model consisting of a wing and a tail which produced vortices of the opposite sign to those of the wing. Thus, the wake is comprised of two symmetric pairs of counter-rotating vortices. The tail vortices are partially wrapping around the tip vortices, and at the same time seem to be undergoing a cooperative instability. The accompanying PIV measurements quantify the interaction of a pair of the counter-rotating vortices. The vortex interaction at the plane of PIV measurements is vigorous, resulting in the enlargement of the wing tip vortex. Confirmation of uniformly progressive enlargement of the tip vortices to facilitate cross-annihilation and eventual quantification of the wake alleviation characteristics could establish this as a practical mechanism.

5. Active schemes

Crow himself proposed a scheme of hastening the development of the Crow instability within a counter-rotating vortex pair, hence accelerating the demise of the wake vortices, by modulating the lift distribution while keeping the total lift constant [23]. Bilanin and Widnall's experiments explored the effect of Crow's suggestion on the stability characteristics of a vortex pair [24].

However, their experiments were confined to the near wake and no vortex ring formation was reported (Table 2). A scheme that has been proposed and successfully tested in the laboratory is that described by Crouch, Rennich and Lele, and Crouch et al. [38,80,81]. In this scheme, selected instability modes within two pairs of symmetric co-rotating vortices are forced to achieve accelerated destruction of the wake vortex system.

5.1. Modulated lift distribution

Crouch et al. [38] have successfully demonstrated in a tow tank an active control system to breakup a four-vortex wake comprised of two symmetric pairs of co-rotating vortices with $\gamma = 0.35$. The system representative of the trailing vortices behind an aircraft in a flaps-down configuration which generated a wake with symmetric co-rotating vortex pairs. The scheme is highlighted in Fig. 4. This scheme has its foundation in the theoretical studies of Crouch [80] and Rennich and Lele [81] that describe the detailed instability mechanics in multiple vortex pair systems. Fig. 4(a) shows a sample result from those calculations. The instability is forced by a symmetric excitation scheme of the control surfaces, preserving total lift and symmetry (Fig. 4(b), (c)). Flow visualization experiments using a generic airplane model in a towing tank have successfully demonstrated the rapid formation of vortex rings (Fig. 4(d)). Markedly shorter vortex linking times were observed in these experiments using acceptable forcing amplitudes (Fig. 4(d)). The vortices resulting from the tail-loading shorten this linking time by increasing separation between the wing tip and flap vortices, providing an additional variable for wake vortex control [39].

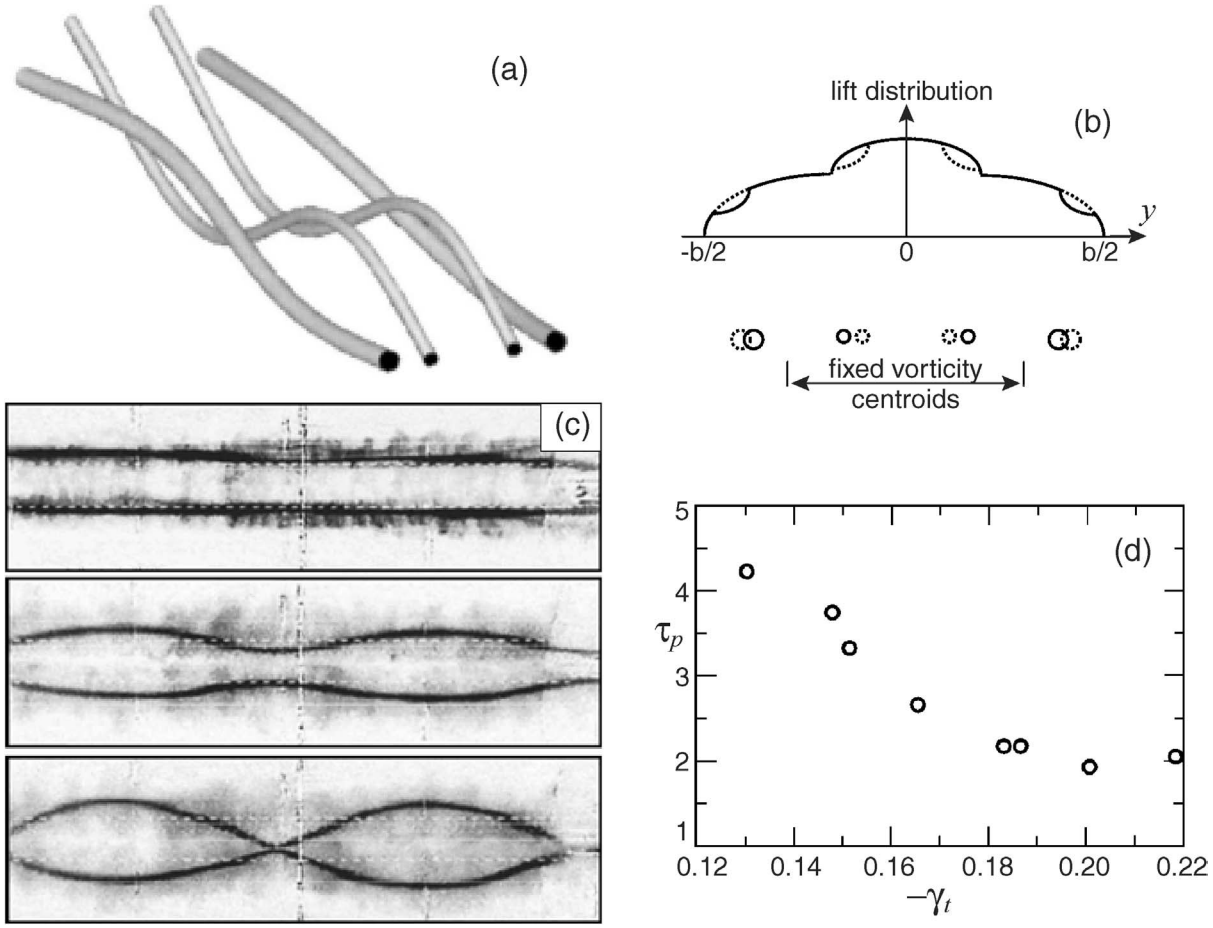

Fig. 4. Active wake alleviation based on modulated lift distribution and its wake comprising of two corotating vortex pairs [38] (reproduced with permission). (a) Sample of computational result showing growth of long wavelength symmetric instability mode. (b) Modulated lift distribution, shifting between solid and dashed configurations. Note that centroids of the vorticity on either side of the wind remain fixed. (c) Flow visualization sequence showing the pinching of vortices. (d) Dimensionless pinch times as a function of the relative strength of the tail vortex.

5.2. Forced vortex filaments

In contrast to forcing the complete wake, vortices may be forced individually to alter the behavior of the vortices individually or in en mass. Of the methods experimented with, continuous or pulsatile jets in vortex cores have received much attention. Another intriguing one is modulating the strength of a vortex by altering the force on its progenitor, by either oscillating or deforming it.

Jacob et al. [49] observe that forcing increases both the separation of a counter rotating vortex pair and the growth rate of the vortex core. Their measurement are made at $C_{\dot{m}} \sim \mathcal{O}(10^{-5})$ and $C_{\mu} \sim \mathcal{O}(10^{-4})$. At low frequencies, these effects are monotonic with increasing forcing frequency. At high frequencies, their measurements suggest a complex response to forcing. This complexity arises from the multitude of possible modes of excitation of the vortices at both short and long wave lengths. Based on measurements and observations, some parameters of importance are suggested in exploring possible means of controlling the behavior of the vortex wake. Those suggestions, however, have not been followed through.

Heyes and Smith [48] present an investigation of pulsed wing-tip jets to introduce cyclic spatial perturbation into a single tip vortex. Their measurement are made at $C_{\dot{m}} \sim \mathcal{O}(10^{-3})$ and $C_{\mu} \sim \mathcal{O}(10^{-2})$. They demonstrated that vortex structure, growth rate, and trajectory could all be altered through forcing with jets. The scheme shows promise for exciting instability in multiple vortex wakes.

Quackenbush et al. [63,87,88] describe a prototype Shape Memory Alloy (SMA)-actuated deformable foil in a vortex wake control scheme for lifting surfaces, named *vortex leveraging*. Actuation is achieved by energizing SMA wires embedded in the skin of the foil to deform it, hence change its aerodynamic characteristics dynamically. The scheme is said to be suitable for both aircraft and submarine applications even though no model or prototype results seems to available in the open literature.

6. Discussion

The primary challenge of the passive wake alleviation concept proposed by the Berkeley group is that of structural modifications. In its present form this wake alleviation concept operates by increasing the outboard loading on the wing, which generates a larger bending moment in the wing. If this design were incorporated into an airplane, the increased bending moment would have to be compensated by strengthening the wing. For this reason the use of outboard flaps would best be employed on a new aircraft design and not an existing one. Perhaps, a means of circumventing this shortcoming is to use other designs, such as vertically oriented flaps [47] or the horizontal stabilizer [19,72], to generate oppositely signed control vortices. Despite the challenges, this wake alleviation concept does possess several advantages. The first is that it is completely passive. It relies on the amplification of the most unstable modes of inherently present perturbations in a real vortex system. Requiring no oscillating flaps or pulsed jets, the triangular-flapped wing design functions by simply placing oppositely signed vortices inboard of the tip vortices and using their presence to disrupt the coherence of the wake. The second advantage of this concept is that the instability between the flap and tip vortices evolves very rapidly when compared to the Crow instability, which requires a few hundred spans to develop, making it a less attractive candidate for rapid wake attenuation. The primary reason for this slow growth rate is that the large spacing between the tip vortices reduces the rate of strain that they induce on each other. By reducing the distance between oppositely signed vortices, the instability can grow more rapidly. Once the instability is triggered, the nonlinear effects overwhelm the flow, which transforms the wake into a three-dimensional one within 20–50 wing spans. The third advantage of this wake alleviation concept is that, although it is passive, its design does allow for the control of the nonlinear evolution of the wake. By varying the relative circulation strength of the flap vortices γ from -0.4 to -0.7 in quiescent background in the tow tank, it has been observed that the behavior of the vortex wake can be widely altered. For smaller values of $|\gamma|$, there is a large exchange of vorticity across the wing centerline in the form of vortex rings. For larger values of $|\gamma|$, the vortices are confined to each side of the wake, and the instability leads to an upward ejection of vorticity. Therefore, depending on the type of behavior desired in the vortex wake and the background flow conditions; such as wind shear, stratification, crosswinds, and turbulence; the strength of the flap vortices can be individually adjusted to direct the vortical activity in the wake. To achieve this freedom in controllability, the behavior of this instability under varying background conditions must be delineated.

The active modulation of the wing loading to hasten the demise of the vortex wake has several issues that have to be addressed before implementation. A criterion of acceptability is needed to decide at what level does the wake system become acceptable. In fact this metric is of global concern and may best be addressed by regulatory organizations. The control scheme relies on the global participation of the vortex system. Background atmospheric conditions such as shear, wind, stratification, even the ground effect, does break the symmetry of the system, hence the excitations needed to achieve the alleviation goal. It is therefore necessary to establish the sensitivity of the scheme to asymmetric background and establish if either side of the vortex wake can be controlled separately. This will also include environmental effects and ground effects. Structural issues brought about by oscillating bending moment in the wing structure are topics that must be addressed, but falls outside this discussion.

Suggestions using pulsed jets or shape memory alloys, or oscillation auxiliary control surfaces are still at their infancy; there does not seem to be reasonably complete laboratory demonstrations on complete wakes. It is however, anticipated that, similar issues raised above will be pertaining to these cases as well.

The Re_Γ for a typical large aircraft is $\mathcal{O}(10^7)$ whereas those for a typical laboratory experiments range from to $\mathcal{O}(10^3)$–$\mathcal{O}(10^5)$. The evidence shows that the behavior of vortex systems for $Re_\Gamma \mathcal{O}(10^3$–$10^4)$ is strongly effected by viscous effects; hence, due caution must be exercised in extending those finding to prototype flows. The experiments in wind tunnels are typically confined to the very near field of the flow where the vortex wake is still forming. The formation is typically complete well within $x/b = 10$, whereas dynamics of the wake takes place at distances of $x/b = \mathcal{O}(10^2)$. The core size of trailing vortices for typical commercial air transport is on the order of $\sigma/b = \mathcal{O}(0.1)$. Thus, thicker vortices, generated at low Re_c with separation distances on the order of the vortex core size are not relevant to the issue of vortex wake control. The axial flow in a vortex has strong influence on its stability characteristics. It is likely that this axial flow is Reynolds number dependent since the boundary layers coming off a lifting body do depend of the Reynolds number. Axial flow measurements, especially at higher Reynolds numbers are sparse (e.g., [34]). Therefore, one must consider this lack of information in extending low Reynolds number instability results to prototype scales. Experiments using thick airfoil forms (NACA-0012 seems to be a popular one, including this author) at Reynolds numbers below about 10^5 are poor choices at high angles of attack, due to laminar separation [74]. In fact, NACA-0012 performs better backwards at low Reynolds numbers!

7. Closing remarks

Laboratory experiment should make no attempt to simulate a prototype using detailed models. They are best suitable for exploring fundamentals, for which simplest geometries are most suitable. This functionality of laboratory experiments is not trivial to replicate in prototypes. Both passive and active systems have been demonstrated in the laboratory. The weakness of the robust passive mechanism is that its implementation on current aircraft is not trivial and the strength of the complicated active mechanism is that it can be implemented. The passive system is a vortex wake design demonstration and may be used as guide to design an aircraft where the wake can be engineered into the design. The laboratory demonstrated active system is a control implementation and has the promise of being retrofitable to existing airframes.

The Berkeley mechanism requires a $\gamma \approx -0.4$. While it may not be a practical approach to achieve this with a 4-vortex system, it is possible that a 6-six vortex system may be easier to implement on an aircraft. As opposed to generating the counter rotating vortex off a single generator, such as the tail tip [19,72], it may be reconstituted by the merger of two weaker vortices originating from different locations, such the tail tip and a flap tip. Such combinations of 6-vortex systems may be both easier to implement and better to achieve the desired results since it will allow for a larger parameter space. Novel active concepts should be explored. For example, the scheme presented at WakeNet2-Europe workshop of dynamically altering the lift distribution, hence modulating the wake vortex structure, via separation control over the wing is an intriguing concept [13].

Finally, one can rightly argue that all wake vortex alleviation mechanisms discussed here, passive or active, are the same: they all rely on selective modes of stabilities. In this regard, classification of a mechanism as passive or active becomes subjective. The Berkeley mechanism of Fig. 2 is named by this author as *completely passive*, simply because it achieves a desired result rapidly without any forcing. In fact, one could easily make an active mechanism out of it by forcing each vortex pair seen in Fig. 1(h) at the appropriate frequency to achieve an incoherent vortex wake much sooner than implied in Figs. 2(c), (d). A close examination of the movie sequence from which Fig. 1(h) is extracted suggests that, if one could seed into the vortex pairs a 5% amplitude modulation at the most amplified wavelength, the time to incoherent appearance of the wake as indicated by the dye dispersion would be reduced by one third of that implied in Figs. 2(c), (d). Conversely, the Boeing mechanism shown in Fig. 4 would become a passive one if left alone. However, the time to achieve the desired vortex wake state would be just too long. Currently, all vortex wakes of transport aircraft in quiescent conditions are decaying through a completely passive mechanism: the Crow instability.

Acknowledgements

I have benefited greatly from a careful review by Gregory D. Miller of The Boeing Company. Victoria Sturgeon of UC Berkeley made numerous editorial corrections. The author acknowledges the continuing support of NASA Ames Research Center.

References

[1] F.W. Caldwell, E.N. Fales, NACA Report 83, 1921.

[2] N.A.V. Piercy, J. Roy. Aero. Soc. 27 (1923) 488–500.
[3] A. Fage, L.F.G. Simmons, Phil. Trans. Roy. Soc. London Ser. A 225 (7) (1926) 303–330.
[4] F.W. Lanchester, Aerodynamics, Van Nostrand, New York, 1908.
[5] J.H. Olsen, A. Goldburg, M. Rogers (Eds.), Aircraft Wake Turbulence and its Detection, Plenum, New York, 1971.
[6] C.D. Donaldson, A.J. Bilanin, in: R.H. Korkegi (Ed.), AGARDograph 204, 1975.
[7] A. Gessow (Ed.), Wake Vortex Minimization, NASA SP-409, 1976.
[8] NATO-AGARD CP-584, 1996.
[9] P.R. Spalart, Ann. Rev. Fluid Mech. 30 (1998) 107–138.
[10] V.J. Rossow, Prog. Aero. Sci. 35 (6) (1999) 507–660.
[11] T. Gerz, F. Holzäpfel, D. Darracq, Prog. Aero. Sci. 38 (3) (2002) 181–208.
[12] E. Coustols, E. Stumpf, L. Jacquin, F. Moens, H. Vollmers, T. Gerz, AIAA Paper No. 2003-0938, 2003.
[13] http://wwwe.onecert.fr/projets/WakeNet2-Europe, 2005.
[14] J.N. Hallock (Ed.), Wake vortex bibliography http://www.volpe.dot.gov/wv/wv-bib.html, 2005.
[15] http://www.boeing.com, 2005.
[16] R.L. Bristol, J.M. Ortega, P.S. Marcus, Ö. Savaş, J. Fluid Mech. 517 (2004) 331–358.
[17] S.C. Crow, AIAA J. 8 (12) (1970) 2172–2179.
[18] D.L. Ciffone, C. Lonzo Jr., NASA TM X-62,459, 1975.
[19] A.D. Durston, W.S. Walker, D.M. Driver, S.C. Smith, Ö. Savaş, J. Aircraft 42 (3) (2005), in press.
[20] J.M. Ortega, R.L. Bristol, Ö. Savaş, AIAA J. 40 (4) (2002) 709–721.
[21] J.M. Ortega, R.L. Bristol, Ö. Savaş, J. Fluid Mech. 474 (2003) 35–84.
[22] R.L. Bristol, J.M. Ortega, Ö. Savaş, AIAA J. 41 (4) (2003) 741–744.
[23] S.C. Crow, in: J.H. Olsen, A. Goldburg, M. Rogers (Eds.), Aircraft Wake Turbulence and its Detection, Plenum, New York, 1971, pp. 577–583.
[24] A.J. Bilanin, S.E. Widnall, AIAA Paper No. 73-107, 1973.
[25] R.E. Dunham, in: A. Gessow (Ed.), NASA Symposium on Wake Vortex Minimization, NASA SP-409, 1976, pp. 221–249.
[26] V.R. Corsiglia, R.A. Jacobsen, N.A. Chigier, in: J.H. Olsen, A. Goldburg, M. Rogers (Eds.), Aircraft Wake Turbulence and Its Detection, Plenum, New York, 1971, pp. 229–242.
[27] G.R. Baker, S.J. Barker, K.K. Bofah, P.G. Saffman, J. Fluid Mech. 65 (1974) 325–336.
[28] P.R. Bandyopadhyay, D.J. Stead, R.L. Ash, AIAA J. 29 (10) (1991) 1627–1633.
[29] A.J. Bilanin, C.D. Donaldson, R.S. Snedeker, AFFDL-TR-74-90, 1974.
[30] S.A. Brandt, J.D. Iversen, J. Aircraft 14 (12) (1977) 1212–1220.
[31] C. Cerretelli, C.H.K. Williamson, J. Fluid Mech. 475 (2003) 41–77.
[32] C. Cerretelli, C.H.K. Williamson, J. Fluid Mech. 493 (2003) 219–229.
[33] A.L. Chen, J.D. Jacob, Ö. Savaş, J. Fluid Mech. 382 (1999) 155–193.
[34] D.L. Ciffone, K.L. Orloff, AIAA J. 12 (8) (1974) 1154–1155.
[35] V.R. Corsiglia, R.G. Schwind, N.A. Chigier, J. Aircraft 10 (12) (1973) 752–757.
[36] P. Coton, in: Characterization and Modification of Wakes from Lift: Vehicles in Fluids, AGARD, CP-584, 1996, pp. 29:1–12.
[37] D.R. Croom, in: A. Gessow (Ed.), NASA Symposium on Wake Vortex Minimization, NASA SP-409, 1976, pp. 239–368.
[38] J.D. Crouch, G.D. Miller, P.R. Spalart, AIAA J. 39 (12) (2001) 2374–2381.
[39] M.J. Czech, G.D. Miller, J.D. Crouch, M. Strelets, AIAA Paper No. 2004-2149, 2004.
[40] A.C. de Bruin, S.H. Hegen, P.B. Rohne, P.R. Spalart, in: Characterization and Modification of Wakes from Lift: Vehicles in Fluids, AGARD, CP-584, 1996, pp. 25:1–12.
[41] W.J. Devenport, M.C. Rife, S.I. Liapis, G.J. Follin, J. Fluid Mech. 312 (1996) 67–106.
[42] W.J. Devenport, J.S. Zsoldos, C.M. Vogel, J. Fluid Mech. 332 (1997) 71–104.
[43] W.J. Devenport, C.M. Vogel, J.S. Zsoldos, J. Fluid Mech. 394 (1999) 357–377.
[44] W.R. Graham, Aeronautical J. (2002) 403–426.
[45] W.R. Graham, S.W. Park, T.B. Nickels, AIAA J. 41 (9) (2003) 1835–1838.
[46] W.R. Graham, L. David, T. Bertenyi, Aeronautical J. (2005), in press.
[47] S. Haverkamp, G. Neuwerth, D. Jacob, Aerospace Sci. Tech. 7 (5) (2003) 331–339.
[48] A.L. Heyes, D.A.R. Smith, Exp. Fluids 37 (2004) 120–127.
[49] J.D. Jacob, D. Liepmann, Ö. Savaş, in: Characterization and Modification of Wakes from Lift: Vehicles in Fluids, AGARD, CP-584, 1996, pp. 27:1–12.
[50] J.D. Jacob, Ö. Savaş, D. Liepmann, AIAA Paper No. 96-2497, 1996.
[51] J.D. Jacob, Ö. Savaş, D. Liepmann, AIAA J. 35 (2) (1997) 275–280.
[52] L. Jacquin, D. Fabre, P. Geffroy, E. Coustols, AIAA Paper No. 2001-1038, 2001.
[53] L. Jacquin, D. Fabre, D. Sipp, V. Theofilis, H. Vollmers, Aerospace Sci. Tech. 7 (2003) 577–593.
[54] F. Laporte, T. Leweke, AIAA J. 40 (12) (2002) 2483–2494.
[55] T. Leweke, C.H.K. Williamson, J. Fluid Mech. 360 (1998) 85–119.
[56] D.K. Lezius, AIAA J. 12 (8) (1974) 1065–1071.
[57] X. Li, J.D. Jacob, AIAA Paper No. 2000-2219, 2000.
[58] P. Meunier, T. Leweke, Phys. Fluids 13 (10) (2001) 2747–2750.
[59] P. Meunier, U. Ehrensteina, T. Leweke, M. Rossi, Phys. Fluids 14 (8) (2002) 2757–2766.

[60] J.H. Olsen, in: J.H. Olsen, A. Goldburg, M. Rogers (Eds.), Aircraft Wake Turbulence and its Detection, Plenum, New York, 1971, pp. 455–472.
[61] J.M. Ortega, Ö. Savaş, AIAA J. 39 (4) (2001) 750–754.
[62] E. Özger, I. Schell, D. Jacob, J. Aircraft 38 (5) (2001) 878–887.
[63] T.R. Quackenbush, A.J. Bilanin, B.F. Carpenter, in: J.H. Jacobs (Ed.), Proceedings of the SPIE, vol. 3674, The International Society for Optical Engineering, 1999, pp. 84–94.
[64] J.C. Patterson, J. Aircraft 12 (9) (1975) 745–749.
[65] J.C. Patterson, E.C.F.L. Jordan, in: A. Gessow (Ed.), NASA Symposium on Wake Vortex Minimization, NASA SP-409, 1976, pp. 251–270.
[66] J.C. Patterson, E.C. Hastings, F.L. Jordan, in: A. Gessow (Ed.), NASA Symposium on Wake Vortex Minimization, NASA SP-409, 1976, pp. 271–303.
[67] V.J. Rossow, J.N. Sacco, P.A. Askins, L.S. Bisbee, S.M. Smith, J. Aircraft 32 (2) (1995) 278–284.
[68] T. Sarpkaya, AIAA J. 36 (9) (1998) 1671–1679.
[69] I. Schell, E. Özger, D. Jacob, Aerospace Sci. Tech. 4 (2) (2000) 79–90.
[70] J.R. Spreiter, A.H. Sacks, J. Aero. Sci. 18 (1) (1951) 21–32, 72.
[71] D.H. Thompson, J. Aircraft 12 (11) (1975) 910–911.
[72] H. Vollmers, R. Stuff, K.A. Buetefisch, H. Mattner, A. Quast, K.H. Horstmann, G. Calcagno, DLR report (2001) IB-223-2001 A 05, DLR, Göttingen.
[73] F. Bao, H. Vollmers, H. Mattner, Institute of Aerodynamics and Flow Technology, DLR, Göttingen.
[74] E.V. Laitone, AIAA J. 34 (9) (1996) 1941–1942.
[75] L. Prandtl, O.J. Tietjens, Applied Hydo- and Aeromechanics, Dover, New York, 1934.
[76] D.P. Delisi, G.C. Greene, J. Aircraft 27 (11) (1990) 968–971.
[77] M.J. Sholl, Ö. Savaş, AIAA Paper 97-0493, 1997.
[78] V.J. Rossow, in: A. Gessow (Ed.) NASA Symposium on Wake Vortex Minimization, NASA SP-409, 1976, pp. 4–54.
[79] P.G. Saffman, Vortex Dynamics, Cambridge University Press, Cambridge, 1992.
[80] J.D. Crouch, J. Fluid Mech. 350 (1997) 311–330.
[81] S.C. Rennich, S.K. Lele, J. Aircraft 36 (2) (1999) 398–404.
[82] D. Fabre, L. Jacquin, A. Loof, J. Fluid Mech. 451 (2002) 319–328.
[83] R. Fjørtoft, Geofysiske Publikasjoner 17 (6) (1950) 2–52.
[84] H. Ludwieg, Z. Flugwiss. 8 (5) (1960) 135–140.
[85] R. Stuff, AIAA Paper 2001-2429, 2001.
[86] R. Stuff, AIAA Paper 2003-1108, 2003.
[87] T.R. Quackenbush, A.J. Bilanin, P.F. Batcho, R.M. McKillip Jr., B.F. Carpenter, in: J.M. Sater (Ed.), Proceedings of the SPIE, vol. 3044, The International Society for Optical Engineering, 1997, pp. 134–146.
[88] T.R. Quackenbush, P.F. Batcho, A.J. Bilanin, B.F. Carpenter, in: J.M. Sater (Ed.), Proceedings of the SPIE, vol. 3326, The International Society for Optical Engineering, 1998, pp. 1259–1271.